2013 IEEE/RSJ International Conference on
Intelligent Robots and Systems (IROS)
November 3-7, 2013. Tokyo, Japan

Tension Propagation Analysis of Novel Robotized Surgical Platform for Transumbilical Single-Port Access Surgery

Jongwon Lee, Yong-Jae Kim, Se-gon Roh, Jiyoung Kim, Younbaek Lee,
Jeonghun Kim, Byungjune Choi, and Kyoungsik Roh

Abstract— **In this paper, tension propagation analysis of a newly designed multi-DOF robotic platform for single-port access surgery (SPS) is presented. The analysis is based on instantaneous kinematics of the proposed 6-DOF surgical instrument, and provides the decision criteria for estimating the payload of a surgical instrument according to its pose changes and specifications of a driving-wire. Also, the wire-tension and the number of reduction ratio to manage such a payload can be estimated, quantitatively. The analysis begins with derivation of the power transmission efficiency through wire-interfaces from each instrument joint to an actuator. Based on the energy conservation law and the capstan equation, we modeled the degradation of power transmission efficiency due to 1) the reducer called wire-reduction mechanism, 2) bending of proximal instrument joints, and 3) bending of hyper-redundant guide tube. Based on the analysis, the tension of driving-wires was computed according to various manipulation poses and loading conditions. In our experiment, a newly designed surgical instrument successfully managed the external load of 1kgf, which was applied to the end effector of a surgical manipulator.**

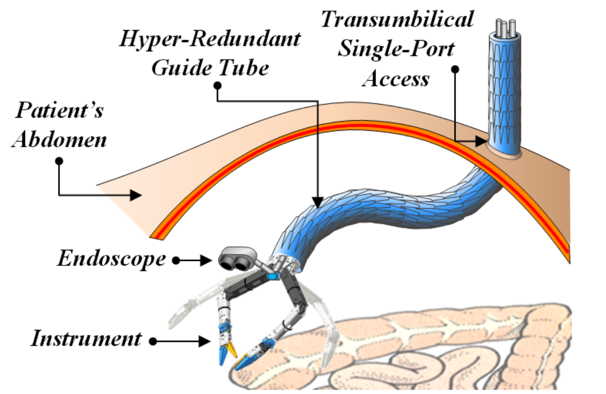

Fig. 1. Conceptual diagram for single-port access surgery (SPS)

I. Introduction

Laparoscopic surgery, also called minimally invasive surgery (MIS), is a surgical technique in which operations in the abdomen are performed through small incision as opposed to the larger incisions needed in conventional laparotomy. It has many advantages such as less invasion, less postoperative pain, better cosmetic result and shorter hospital stay. However, in spite of these merits, surgeon's limited sensory and motor capability concomitant with small incisions made the precise surgical manipulation be more difficult during laparoscopy. With the aid of robot technology, the da Vinci robotic surgical system have improved dexterity, precision, and ergonomics with motion scaling and tremor control during the surgery, so nowadays the robotic multi-port laparoscopic surgery has become the standard in many surgical fields, such as urological and gynecological surgery.

Futher attempts to minimize mobidity of MIS and patient's postoperative pain have resulted in the development of single-port access surgery (SPS). Compared with natural orifice translumenal endoscopic surgery (NOTES), SPS is not totally incisionless surgery. However, it can have the same cosmetic advantages of NOTES, as a single scar gets lost in the umbilicus. Moreover, because i) SPS has no trouble to extract organ specimens after the surgery via the abdomen, ii) SPS has shorter learning curve coupled with familiar laparoscopic views, and iii) SPS is suitable to be transformed into conventional transabdominal laparoscopic surgery more rapidly when failure of operation occurs, SPS has been adopted in lots of clinical applications recently [1]–[4].

However, working with multiple instruments e.g. more than two arms and one endoscope through a single-port to perform complex intra-abdominal procedures brings some difficulties. Passing multiple instruments through the same incision restricts freedom of movement, so that overcrowding and confliction between instruments are inevitable [5]. Although several manual articulated instruments have been developed to assist those SPS and/or NOTES, such as RealHand by Novare Surgical [6], Autonomy Laparoangle by Cambridge Endo [7], Transport by USGI Medical [8], Endo-SAMURAI by Olympus Corp. [9], and DDES by Boston Scientific [10], a workspace of manipulation and a payload still have limitations. They can only be applicable to perform the operation which has low level of difficulty like cholecystectomy in humans [11].

Much research has been conducted to improve SPS with the use of surgical robots for precise manipulation in the abdomen. Xu et al. developed a self-deployable IREP surgical robot for SPS/NOTES which had two backbone type 7-DOF surgical instruments and one 3-DOF endoscope with 15mm outer diameter in folded configuation [12]. Piccigallo et al. developed an embedded motor-driven type SPRINT surgical platform for SPS, which comprised two 6-DOF surgical instruments connecting with a rigid guide tube of 30mm

*This work was supported in part by SAIT of Samsung Electronics

Jongwon Lee, Yong-Jae Kim, Se-Gon Roh, Jiyoung Kim, Younbaek Lee, Jeonghun Kim, Byungjune Choi, and Kyoungsik Roh are with Samsung Advanced Institute of Technology, Ki-hung gu, Yong-in si, Kyunggi do, Rep. of Korea (corresponding author to provide phone: +82-31-280-1587, e-mail: jwon81.lee@samsung.com)

978-1-4673-6357-0/13/$31.00 ©2013 IEEE

diameter [13]. Shang et al. developed a hybrid micro-motor driven robotized surgical platform for SPS/NOTES where two 4-DOF surgical instruments and one 5-DOF articulated endoscope were equipped at the distal-end of a rigid guide tube [14], [15]. Kobayashi et al. developed a surgical robot for SPS which had 2-DOF guide tube and two 5-DOF tissue manipulators [16], [17]. Can et al. developed a hydraulic telemanipulator for SPS, especially for cholecystectomy, which had two 6-DOF surgical instruments and one 5-DOF endoscope with a rigid guide tube of 22mm diameter [18]. Intuitive Surgical Corp. also have developed novel robotic instrument, called VeSPA, for SPS with two curved cannulae, two semi-rigid instruments, and one rigid endoscope [19].

In spite of these efforts, robotic SPS technology has still common limitations like belows. 1) Except for the embedded motor-driven type platform, there was no robotized surgical platform for SPS which satisfied payload requirements of 5-10N to perform various laparoscopic surgeries, while maintaining its MIS scheme. 2) Due to the use of rigid guide tube, most of conventional robotized surgical platform for SPS were not free from the pose constraint at an incision port of umbilicus. The position and the orientation of surgical instruments cannot be set arbitrary inside the abdomen as surgeons wish. The former is related to the functionality of a robot, the letter is related to its usability.

In order to solve these limitation, we sought to devise a novel master/slave telemanipulation system for SPS which characterized like belows

- Small-sized multi-DOF surgical instrument : Total dual 6-DOF surgical instruments (2-DOF shoulder, 1-DOF elbow, 3-DOF wrist, gripper) with the diameter of 8mm and one 3-DOF endoscope (1-DOF neck, 2-DOF head) were newley designed.
- Wire-reduction mechanism embedded in instrument joint : The reducer, called wire-reduction mechanism was equipped in every single joint of a surgical instrument. It can increase the payload and the stiffness of a small-sized surgical instrument significantly, while reducing the tension of a driving wire.
- Hyper-redundant guide tube : Total 4-DOF hyper-redundant guide tube was designed, which was composed of two segments, each segment had 2-DOF rotational motion. It can help a surgical instrument take an arbitrary pose inside the abdomen as surgeons wish, and increase the workspace of the robot to cover the entire space inside the abdomen.

In this paper, based on the mechanisms of the newly designed 6-DOF surgical instrument, the analysis of wire-tension propagation is presented, which considers the wire interface of a surgical instrument. We modeled how the driving wire-tension was changed from each joint of the intrument to the actuator. With the aid of this study, we can provide the decision criteria for estimating the payload of a surgical instrument according to its pose changes and the specification of a driving-wire. Also, the wire-tension or the number of a reduction ratio to withstand such a payload can be estimated quantitatively, so that it can be usefully applied when the specification of the system is determined.

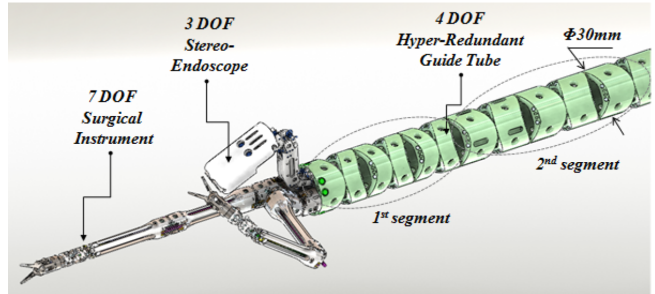

(a)

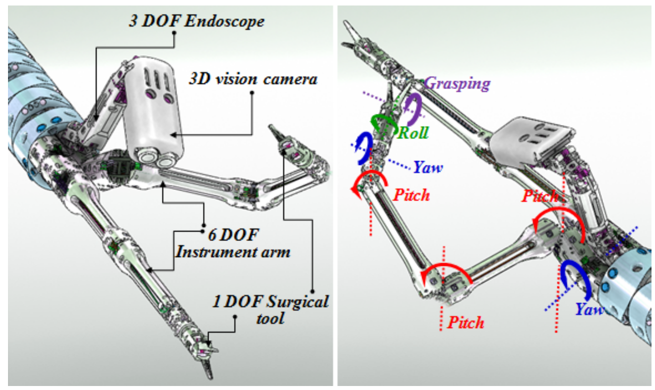

(b)

Fig. 2. System overview of the proposed robotic platform for SPS

The remainder of this paper is organized as follows. We begin by introducing an overview of our robotic system in Section II. In Section III, the detailed setup of an instrument joint is described, and tension propagation analysis is provided. In Section IV, the tension of driving wires is simulated according to various manipulation poses, and verified by experiments. The paper concludes with Section V, which includes a conclusion of the proposed surgical robot and a discussion.

II. The SAIT Robotic System Overview

Fig. 2 represents the system overview of the proposed robotic platform for SPS. The system consists of the following core elements.

- Surgical manipulator : The small-sized dual 6-DOF surgical instruments including a gripper are installed at the end of the hyper-redundant guide tube. It has 2-DOF shoulder, 1-DOF elbow, 3-DOF wrist motions. The diameter of its wrist joint is 8mm.
- Endoscope : The 3-DOF endoscope is also equipped at the end of the hyper-redundant guide tube, so that the functions of mechanical zoom-in, zoom-out, and browsing a surgical site can be implemented.
- Hyper-redundant guide tube : The 4-DOF guide tube with the diameter of 30mm is installed, which consists of two 2-DOF segments. It can help the surgical robot keep the optimal pose for manipulating internal organs

intraoperatively, as well as increase the workspace of the surgical robot inside the abdomen [20].
- Actuation package : The actuation package provides the independent control of the surgical manipulators and the endosocope.

All surgical manipulators and endoscope were actuated by a wire-driven mechanism. The wire (Spectra fiber, Shimano Inc.) is connected from surgical manipulators and the endoscope to the corresponding actuation package. It passes a predefined small channel of a conduit inside the guide tube.

The procedure of the proposed robotic SPS system consists of the following steps.

1) Incision of the patient's umbilicus about 30-35mm and insertion of a trocar;
2) Insertion of an endoscope through an umbilical port, equipped to the end of a hyper-redundant guide tube;
3) Approach to a surgical site using guide tube movement;
4) Insertion of the first/second surgical instrument through the guide tube;
5) Insertion of the third surgical instrument if needed;
6) Perform surgical tasks remotely by using a master device.

The requirements for proposed robotic SPS system were determined after several disccusion with cooperative clinical experts. The overlapping workspace of the manipulators was defined as X:±100mm, Y:±35mm, and Z:±75mm which was enough to perform general laparoscope surgeries. With the aid of the guide tube movement, the workspace of the proposed system can be more extended to the level, which covers the entire volume inside the patient's abdomen. The payload was defined as 1kgf at the forward-straight pose of a surgical manipulator, to raise heavy organs like a liver during the surgery.

III. Tension Propagation Analysis

In order to analyze the tension propagation via wire-interfaces of a surgical instrument, its instantaneous kinematics becomes the prerequisite information. In this section, based on the kinematic configuation of the newly designed sugical manipulator and its Jacobian, we will discuss the tension propagation analysis in order.

A. Kinematics of Surgical Instrument

Fig. 3 represents the schematic drawing of the manipulator that shows the kinematic configuration of our proposed surgical manipulator. It has total 6-DOF joint space which consist of shoulder-yaw, shoulder-pitch, elbow-pitch, wrist-pitch, wrist-yaw, wrist-roll, plus grasper in order. Due to the shoulder and elbow configurations, we can manipulate the surgical tasks precisely, while alleviating the triangulation problem which is the common limitation of conventional manual SPS/NOTES platforms. Instead of general revolute joints, each joint of the newly designed surgical manipulator possesses the rolling joint. Although the derivation of its kinematics brought to be complex formulation, the rolling joint can effectively mitigate the slack of a driving wire depending on manipulation pose changes.

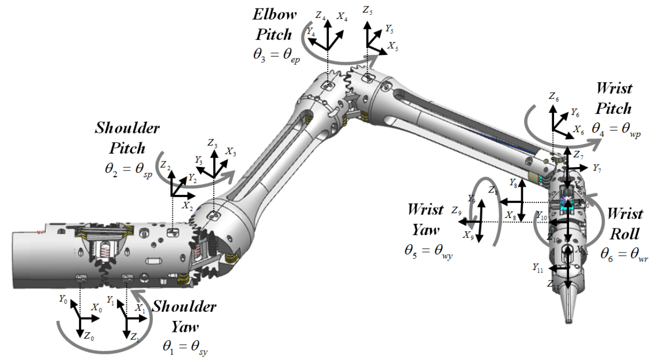

Fig. 3. Schematic drawing of one instrument showing the kinematic configuration

TABLE I
INSTRUMENT KINEMATIC PARAMETERS (DH NOTATION)

Joint	a_i	α_i	d_i	θ_i
1	a_1	0	0	$\theta_1/2$
2	a_2	90	0	$\theta_1/2$
3	a_3	0	0	$\theta_2/2$
4	a_4	0	0	$\theta_2/2$
5	a_5	0	0	$\theta_3/2$
6	a_6	0	0	$\theta_3/2$
7	a_7	0	0	$\theta_4/2$
8	a_8	-90	0	$\theta_4/2$
9	a_9	0	0	$\theta_5/2$
10	0	90	0	$90+\theta_5/2$
11	0	0	d_{11}	θ_6

All angles in degrees.

For the determination of the instantaneous kinematics, we treated every hinge of the manipualtor as an independent joint. As shown in Fig. 3, total 11 independent joints were proposed subsequently. The DH (Denavit-Hartenberg) parameters for each joint were defined in Table I. A composite homogeneous transformation matrix, ${}^{i-1}\mathbf{T}_i$, can be found to be

$$
{}^{i-1}\mathbf{T}_i = \begin{bmatrix} \cos\theta_i & -\cos\alpha_i \sin\theta_i & \sin\alpha_i \sin\theta_i & a_i \cos\theta_i \\ \sin\theta_i & \cos\alpha_i \cos\theta_i & -\sin\alpha_i \cos\theta_i & a_i \sin\theta_i \\ 0 & \sin\alpha_i & \cos\alpha_i & d_i \\ 0 & 0 & 0 & 1 \end{bmatrix} \tag{1}
$$

Consequently, the forward kinematics is calculated as follows

$$
{}^0\mathbf{p} = {}^0\mathbf{T}_1 \cdot {}^1\mathbf{T}_2 \cdot {}^2\mathbf{T}_3 \cdot {}^3\mathbf{T}_4 \cdots {}^{11}\mathbf{T}_{12} \cdot \begin{bmatrix} 0 \\ 0 \\ 0 \\ 1 \end{bmatrix} \tag{2}
$$

where ${}^0\mathbf{p}$ represents task-space vectors of the end effector, expressed in the reference frame Σ_0. Assuming the 3-dimensional task-space vector of the end effector is $\mathbf{X}$ relevant to the first 3 rows of ${}^0\mathbf{p}$, and the 6-dimensinal joint-space vector is $\boldsymbol{\theta} = [\theta_1, \theta_2, \cdots, \theta_6]^{\mathrm{T}}$, the Jacobian can be calculated as

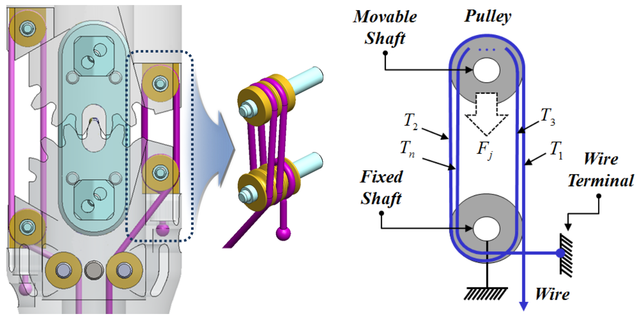

(a) (b)

Fig. 4. Wire-reduction mechanism (a) a pair of wire-reduction mechanism embedded at elbow's rolling joint and (b) schematic diagram of wire-reduction when the number of a reduction ratio is n.

$$\mathbf{J}(\theta) = \frac{\partial \mathbf{X}}{\partial \theta^{\mathrm{T}}} = \begin{bmatrix} \frac{\partial X_1}{\partial \theta_1} & \frac{\partial X_1}{\partial \theta_2} & \cdots & \frac{\partial X_1}{\partial \theta_6} \\ \frac{\partial X_2}{\partial \theta_1} & \frac{\partial X_2}{\partial \theta_2} & \cdots & \frac{\partial X_2}{\partial \theta_6} \\ \frac{\partial X_3}{\partial \theta_1} & \frac{\partial X_3}{\partial \theta_2} & \cdots & \frac{\partial X_3}{\partial \theta_6} \end{bmatrix} \in \Re^{3x6} \tag{3}$$

Although the derivation of the Jacobian is straight-forward based on the above forward kinematics, detailed derivation of the Jacobian matrix is omitted in here, because of its complex formulation.

B. Tension Propagation Analysis

The proposed robotic SPS platform is designed to be actuated by a wire-driven mechanism. After going by 1) wire-reduction mechanism, the wire passes through bending sections caused by 2) joint interfaces of a surgical instrument and 3) hyper-redundant guide tube. Because of these components inducing the friction via wire-paths, the actuation force to manipulate surgical tasks while enduring the external loads becomes to be amplified. In this section, we will discuss the analysis of wire tension propagation, which considers the power trasmission efficiency of the above three elements of wire-paths.

1) Efficiency degradation by wire-reduction mechanism: The proposed robotized surgical platform for SPS retained the reducer, called wire-reduction mechanism, in every single joint of a surgical instrument. As shown in Fig. 4, understanding the function of a movable pulley serves as an insight in invention of the wire-reduction mechanism. Fig. 4(a) showes a pair of the wire-reduction mechanism embedded at the rolling elbow-yaw joint, and Fig. 4(b) showes a schematic diagram of wire-reduction when the reduction ratio becomes $n:1$. The idea can increase the payload and the stiffness of a small-sized surgical instrument significantly, while reducing the average tension of a driving wire.

In case that miniature pulleys are used in the wire-reduction mechanism, the power transmission efficiency of a wire-reduction mechanism via the pulley, η, can be computed based on the energy conservation law as follows

$$(T_2 \cdot D/2)\,\theta_{rot} = (T_1 \cdot D/2 - T_{sum} \cdot \mu \cdot d/2)\,\theta_{rot} \tag{4}$$

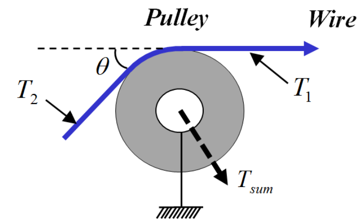

Fig. 5. Schematic diagram of wire interface at each upper joint of a surgical instrument.

where T_1 and T_2 is the tension of a driving wire at the force input terminal, and that of a driven wire at the force output terminal via the pulley, respectively. T_{sum} via a pulley becomes $T_1 + T_2$. D and d is the outer diameter and the inner diameter of a pulley, respectively. μ and θ_{rot} is the Coulomb friction coefficient between the inner-surface of a pulley and a shaft, and the rotation angle of a pulley, respectively. Thus the efficiency of a wire-reduction mechanism, η, via a pulley can be found to be

$$\eta = \frac{T_2}{T_1} = \left(\frac{D - d\mu}{D + d\mu}\right) \tag{5}$$

Based on the power transmission efficiency of a wire-reduction mechanism, the corresponding j-th joint force between two shafts when the number of a wire-reduction is n, F_j, can be calculated as follows

$$\begin{aligned} F_j &= \sum_{i=1}^{n} T_i = T_1 + T_2 + T_3 + \cdots + T_n \\ &= T_1 + \eta T_1 + \eta T_2 + \cdots + \eta T_{n-1} \\ &= T_1 + \eta T_1 + \eta^2 T_1 + \cdots + \eta^{n-1} T_1 \\ &= \left(\frac{1 - \eta^n}{1 - \eta}\right) T_1 \end{aligned} \tag{6}$$

The wire tension to withstand the j-th joint force between two shaft at the end-terminal of a wire-reduction mechanism, T_{wr}^{j}, becomes as follows

$$T_{wr}^{j} = T_1 = \left(\frac{1 - \eta}{1 - \eta^n}\right) F_j \tag{7}$$

2) Efficiency degradation by wire-interface at the surgical instrument: After going by wire-reduction mechanism, the wire passes through the bending section caused by the upper joint configuration of a surgical instrument. As shown in Fig. 5, T_{sum} can be computed by the second law of Cosines with respect to the bending angle of a wire as follows

$$T_{sum} = \sqrt{T_1^2 + T_2^2 - 2T_1 T_2 \cos\theta} \tag{8}$$

Based on the Eqn. (4) and (8), the input tension of a wire can be derived as below

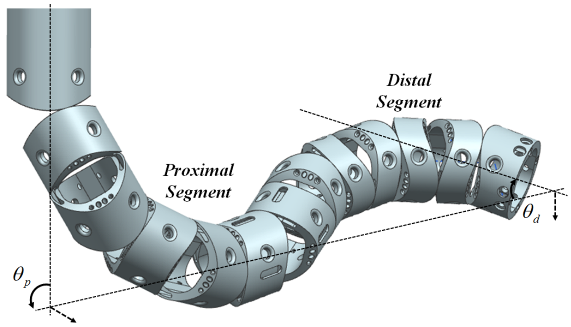

Fig. 6. Bending of the hyper-redundant guide tube of the proposed robotic SPS platform.

$$T_1 = \frac{\left(D^2 T_2 - \mu^2 d^2 T_2 \cos\theta\right)}{D^2 - \mu^2 d^2} \pm \frac{\sqrt{\left(D^2 T_2 - \mu^2 d^2 T_2 \cos\theta\right)^2 - \left(D^2 - \mu^2 d^2\right)^2 T_2^2}}{D^2 - \mu^2 d^2} \quad (9)$$

The power transmission efficiency via a interface pulley with respect to the bending angle of a wire, $\eta(\theta) \in [0,1]$, can be obtained as follows

$$\eta(\theta) = \frac{T_2}{T_1} = \frac{D^2 - \mu^2 d^2}{(D^2 - \mu^2 d^2 \cos\theta) + \sqrt{\left(D^2 - \mu^2 d^2 \cos\theta\right)^2 - \left(D^2 - \mu^2 d^2\right)^2}} \quad (10)$$

which is identical with Eqn. (5) when the bending angle of a wire becomes 180°.

Therefore, the resulting wire tension to withstand the joint force of T^j_{wr} at the end-terminal of a surgical manipulator considering the rolling joint, $T^j_{toolend}$, becomes as follows

$$T^j_{toolend} = T^j_{wr} \cdot \left(\prod_{i=j}^{7} \frac{1}{\eta(\theta_i/2)^2} \right) \cdot \frac{1}{\eta(\pi)} \quad (11)$$

where j is the index of the corresponding joint, defined as 7 at the shoulder-yaw joint, 6 at the shouler-pitch joint, 5 at the elbow-pitch joint, 4 at the wrist-pitch joint, 3 at the wrist-yaw and roll joint. The squared dominator of the $\eta(\theta)/2$ is due to the rolling joint of a surgical manipulator.

3) Efficiency degradation by wire-interface at the hyper-redundant guide tube: In order to transfer the power from the actuation package to the surgical manipulator, the wire passed through the predefined small channel of a teflon conduit located inside the hyper-redundant guide tube. The degradation of the power transmission efficiency by bending of the 4-DOF guide tube can be modeled as the combination of the efficiency degradation caused by two large capstans. The wire tension at the end-terminal of a guide tube, $T^j_{actuator}$, can be derived as follows

$$T^j_{actuator} = T^j_{toolend} \cdot e^{\mu'\left(\theta_d + \theta_p\right)} \quad (12)$$

where θ_d, and θ_p is the bending angle of a distal and proximal segment of a guide tube in each bending plane, respectively. μ' is the Coulomb friction coefficient between the inner surface of a teflon conduit and a driving wire.

Therefore, based on Eqn. (7), (11), (12), the resulting wire tension at the end-terminal of a guide tube can be computed to be

$$\begin{aligned} &T^j_{actuator}(n, \theta_i, \theta_d, \theta_p) \\ &= F_j \cdot \frac{1-\eta(\pi)}{1-\eta(\pi)^n} \cdot \prod_{i=j}^{7} \frac{1}{\eta(\theta_i/2)^2} \cdot \frac{1}{\eta(\pi)} \cdot e^{\mu'\left(\theta_d+\theta_p\right)} \\ &= \frac{J_j^T F_{ext}}{r_j} \cdot \frac{1-\eta(\pi)}{1-\eta(\pi)^n} \cdot \prod_{i=j}^{7} \frac{1}{\eta(\theta_i/2)^2} \cdot \frac{1}{\eta(\pi)} \cdot e^{\mu'\left(\theta_d+\theta_p\right)} \end{aligned} \quad (13)$$

where J_j is the j-th column in Jacobian of the manipulator, F_{ext} is the external load which is applied at the end effector of the proposed robotic SPS platform in the reference frame Σ_0, r_j is the length of the moment arm at the corresponding joint between the center plane and the shaft where F_j is applied.

IV. Simulation and Experiment

Based on the Eqn. (13), the tension of a driving wire was computed according to manipulation pose changes of a surgical instrument. As shown in Fig. 7, the standard pose for general surgical manipulation considering the triangulation ($\theta_1 = 0°$, $\theta_2 = -45°$, $\theta_3 = 90°$, $\theta_4 = -45°$, $\theta_5 = 0°$) and the straight-forward pose for the most extreme case in a view point of a payload ($\theta_1 = 0°$, $\theta_2 = 0°$, $\theta_3 = 0°$, $\theta_4 = 0°$, $\theta_5 = 0°$) were chosen as representative poses for surgical manipulation. Assuming the various loads were applied to the end effector of a surgical manipulator with respect to the reference coordinate Σ_0, the tension of a driving wire was estimated, at the predefined location of the proposed robotic SPS system.

Table II shows the simulation results of tension propagation. Assuming $\mu = 0.13$, $\mu' = 0.1$, $n = 4$, $\theta_d = 90°$, and $\theta_p = 90°$, the tension of F_j, T_{wr}, $T_{toolend}$, and $T_{actuator}$ relating the corresponding joint were estimated. Parameters of μ and μ' were obtained by the experiment. And, bending angles of a guide tube were chosen, considering its maximum joint angle. The tension becomes to be increased after passing the latter wire intefaces, due to the degradation of a power transmission efficiency. The larger the bending angle of a driving wire is, the more the increment becomes. The maximum joint force at the surgical manipulator, F_j, reaches 226.8N at the shoulder-yaw joint, when the surgical manipulator is in the straight-forward pose and its loading condition is (0, 10N, 0). Fig. 8 illustrates the comparison result at this extreme case in a view point of payload. Because the maximum joint force, F_j, reaches 226.8N which is beyond the minimum breaking strength of a steel cable used in general MIS

TABLE II

SIMULATION RESULTS OF DRIVING-WIRE TENSION PROPAGATION WHEN $\mu = 0.13$, $\mu' = 0.1$, $n = 4$, $\theta_d = 90^\circ$, AND $\theta_p = 90^\circ$.

Estimated Values Per Joint	Configuration 1 (Standard Pose)					Configuration 2 (Straight-Forward Pose)					Loading Conditions
	Wrist Yaw	Wrist Pitch	Elbow Pitch	Shoulder Pitch	Shoulder Yaw	Wrist Yaw	Wrist Pitch	Elbow Pitch	Shoulder Pitch	Shoulder Yaw	
F_j	0N	2.39N	63.9N	0N	0N	0N	0N	0N	0N	0N	(10N, 0, 0)
T_{wr}	0N	0.73N	19.6N	0N	0N	0N	0N	0N	0N	0N	
$T_{toolend}$	0N	1.08N	25.9N	0N	0N	0N	0N	0N	0N	0N	
$T_{actuator}$	0N	1.48N	35.4N	0N	0N	0N	0N	0N	0N	0N	
F_j	45.5N	0N	0N	0N	185.8N	45.5N	0N	0N	0N	226.8N	(0, 10N, 0)
T_{wr}	14.0N	0N	0N	0N	57.0N	14.0N	0N	0N	0N	69.5N	
$T_{toolend}$	21.8N	0N	0N	0N	63.6N	17.4N	0N	0N	0N	77.7N	
$T_{actuator}$	29.8N	0N	0N	0N	87.1N	23.8N	0N	0N	0N	106.3N	
F_j	0N	70.7N	124.2N	158.1N	0N	0N	71.1N	149.9N	198.5N	0N	(0, 0, 10N)
T_{wr}	0N	21.7N	38.1N	48.5N	0N	0N	21.8N	46.0N	60.9N	0N	
$T_{toolend}$	0N	32.0N	50.3N	60.5N	0N	0N	27.2N	57.4N	76.0N	0N	
$T_{actuator}$	0N	43.8N	68.8N	82.8N	0N	0N	37.2N	78.5N	104.0N	0N	

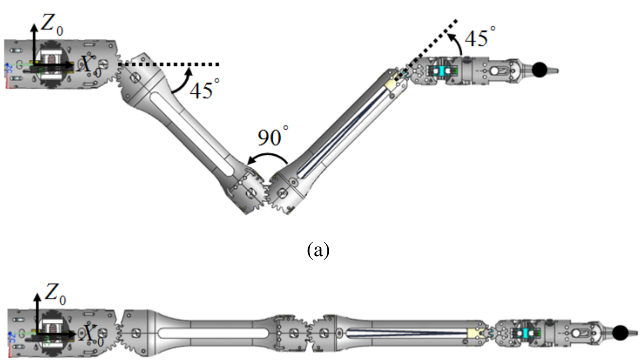

Fig. 7. Two representative poses of the surgical manipualtor used for tension propagation simulation (a) standard pose and (b) straight-forward pose.

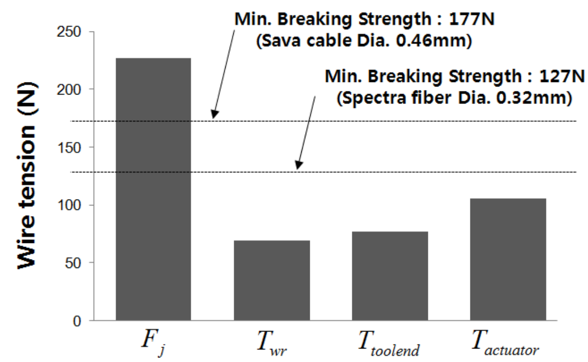

Fig. 8. Comparison with the tension of a shoulder-yaw joint wire depending on the location of a wire-path, when the surgical manipulator is in the straight-forward pose, its loading condition is (0,10N,0), and its reduction ratio is 4:1.

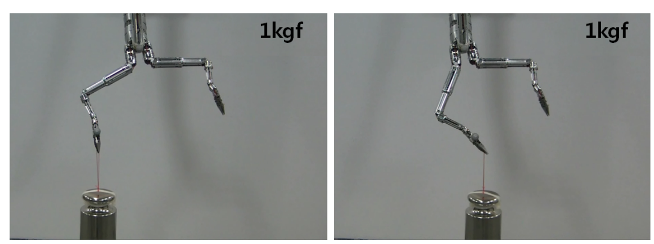

Fig. 9. Results of a payload experiment, when the load condition is 1kgf.

surgical instruments, such a load cannot be managed by using conventional cable-driven mechanisms.

Obviously, this value is too much for conventional wire-driven surgical robot platforms to manage, while maintaining its MIS scheme. Managing such a joint torque is a bottleneck in developing the small-sized multi-DOF surgical instrument with the diameter less than 8mm. By using the 4:1 wire-reduction mechanism, our robotic platform can effectively reduce its wire tension to 106.3N at an actuator. Based on the above simulation, we set the wire reduction ratio to be 4:1, the diameter of the wire to be 0.32mm, which breaking strength became 24kg in the static state, and 13kg in the dynamic state. As shown in Fig. 9, we conducted the payload experiment when the load condition is 1kgf based on FLS (Fundamentals of Laparoscopic Surgery) standard. In our experiment, the payload test to manage the external load of 1kgf at the end effector was successfully performed with above specifications. By adjusting the reduction ratio and the wire thickness, we expect that the payload of a surgical manipulator can be enhanced much more than 1kgf even at the surgical instrument with the diameter less than 8mm.

V. CONCLUSION

In this paper, we presented tension propagation analysis for the newly designed wire-driven multi-DOF robot-assisted SPS platform. Major contribution of this paper is that the analysis can provide a novel decision criteria for estimating the payload of a surgical instrument according to its pose changes and detailed specifications of wire-driven instrument mechanism, quantitatively.

Based on instantaneous kinematics of the proposed 6-DOF surgical manipulator, the tension of a driving wire was modeled according to two representative manipulation pose changes. Based on the energy conservation principle at the pully interface, we derived the power transmission efficiency via the wire-reduction mechanism and bending of proximal joints of a surgical manipulator. Assuming the motion of a hyper-redundant guide tube to be the combination of two large capstans, we also modeled the power transmission efficieny via bending of a 4-DOF hyper-redundant guide tube. Based on those three elements consisting of the wire-interface, the resulting tension of a driving-wire was derived at the predefined location of the proposed robotic SPS system. By using our tension propagation models, we set the detailed specifications of our robot-assisted SPS platform. In our experiment, managing the external load of 1kgf at the end effector was successfully conducted.

As a future work, the evaluation of tension propagation modeling will be followed by experiments. Also, the detailed disscussion about the effectiveness and upper limit of a reduction ratio will be performed with respect to the degradation of power transmission efficiency via wire-interfaces.

REFERENCES

[1] G. Navarra, E. Pozza, S. Occhionorelli, P. Carcoforo, and I. Donini, "One-wound laparoscopic cholecystectomy," *British Journal of Surgery*, Vol. 84, Issue 5, pp. 695, 1997.

[2] A. D'Alessio, E. Piro, B. Tadini, and F. Beretta, "One-Trocar Transumbilical Laparoscopic-Assisted Appendectomy in Children: Our Experience," *European Journal of Pediatric Surgery*, Vol. 12, Issue 1, pp. 24-7, 2002.

[3] A. A. Saber, M. H. Elgamal, E. A. Itawi, and A. J. Rao, "Single Incision Laparoscopic Sleeve Gastrectomy (SILS): A Novel Technique," *Obesity Surgery*, Vol. 18, Issue 10, pp. 1338-42, 2008.

[4] W. M. White, G. P. Haber, R. K. Goel, S. Crouzet, R. J. Stein, and J. H. Kaouk, "Single-port Urological Surgery: Single-center Experience With the First 100 Cases," *Urology*, Vol. 74, Issue 4, pp. 801-4, 2009.

[5] J. H. Kaouk, R. K. Goel, G. P. Haber, S. Crouzet, and R. J. Stein, "Robotic Single-Port Transumbilical Surgery in Humans: Initial Report," *BJU International*, Vol. 103, Issue 3, pp. 366-9, 2009.

[6] J. D. Raman, K. Bensalah, A. Bagrodia, J. M. Stern, and J. A. Cadeddu, "Laboratory and Clinical Development of Single Keyhole Umbilical Nephrectomy," *Urology*, Vol. 70, Issue 6, pp. 1039-42, 2007.

[7] Autonomy Laparo-Angle^{TM}. Instruments from Cambridge Endo. http://www.cambridgeendo.com/instruments/autonomy-laparo-angle.php

[8] L. Swanstrom, P. Swain, and P. Dent, "Development and validation of a new generation of flexible endoscope for NOTES," *Surgical Innovation*, Vol. 16, No. 2, pp. 104-10, 2009.

[9] G. O. Spaun, B. Zheng, and L. L. Swanstrom, "A multitasking platform for natural orifice translumenal endoscopic surgery (NOTES): a benchtop comparison of a new device for flexible endoscopic surgery and a standard dual-channel endoscope," *Surgical Endoscopy*, Vol. 23, Issue 12, pp. 2720-7, 2009.

[10] C. C. Thompson, M. Ryou, N. J. Soper, E. S. Hungess, R. I. Rothstein, and L. L. Swanstrom, "Evaluation of a manually driven, multitasking platform for complex endoluminal and natural orifice transluminal endoscopic surgery applications (with video)," *Gastrointestinal Endoscopy*, Vol. 70, Issue 1, pp. 121-5, 2009.

[11] S. N. Shaikh and C. C. Thompson, "Natural Orifice Translumenal Surgery: Flexible Platform Review," *World Journal of Gastrointestinal Surgery*, Vol. 2, Issue 6, pp. 210-6, 2010.

[12] K. Xu, R. E. Goldman, J. Ding, P. K. Allen, D. L. Fowler, and N. Simaan, "System Design of an Insertable Robotic Effector Platform for Single Port Access (SPA) Surgery," *IEEE/RSJ International Conference on Intelligent Robots and Systems*, St. Louis, USA, 2009, pp. 5546-52.

[13] M. Piccigallo, U. Scarfogliero, C. Quaglia, G. Petroni, P. Valdastri, A. Menciassi, and P. Dario, "Design of a Novel Bimanual Robotic System for Single-Port Laparoscopy," *IEEE/ASME Transactions on Mechatronics*, Vol. 15, No. 6, pp. 871-8, 2010.

[14] D. P. Noonan, V. Vitiello, J. Shang, C. J. Payne, and G. Z. Yang, "A Modular, Mechatronic Joint Design for a Flexible Access Platform for MIS," *IEEE/RSJ International Conference on Intelligent Robots and Systems*, San Francisco, USA, 2011, pp. 949-54.

[15] J. Shang, C. J. Payne, J. Clark, D. P. Noonan, K. Kwok, A. Darzi, and G. Z. Yang, "Design of a Multitasking Robotic Platform with Flexible Arms and Articulated Head for Minimally Invasive Surgery," *IEEE/RSJ International Conference on Intelligent Robots and Systems*, Vilamoura, Portugal, 2012, pp. 1988-93.

[16] Y. Kobayashi, Y. Tomono, Y. Sekiguchi, H. Watanabe, K. Toyoda, K. Konishi, M. Tomikawa, S. Ieiri, K. Tanoue, M. Hashizume, and M. G. Fujie, "A Surgical Robot with Vision Field Control for Single Port Endoscopic Surgery," *International Journal of Medical Robotics and Computer-Assisted Surgery*, Vol. 6, Issue 6, pp. 454-64, 2010.

[17] T. Noguchi, Y. Kobayashi, K. Kawamura, H. Watanabe, Y. Tomono, Y. Sekiguchi, H. Seno, K. Toyoda, M. Hashizume, and M. G. Fujie, "Application of Control Modes of a Master Manipulator for a Robotic System to Assist with Single Port Endoscopic Surgery," *IEEE/RSJ International Conference on Intelligent Robots and Systems*, Vilamoura, Portugal, 2012, pp. 1270-6.

[18] S. Can, C. Staub, A. Knoll, A. Fiolka, A. Schneider, and H. Feussner, "Design, Development and Evaluation of a Highly Versatile Robot Platform for Minimally Invasive Single-Port Surgery," *IEEE RAS/EMBS International Conference on Biomedical Robotics and Biomechatronics*, Roma, Italy, 2012, pp. 817-22.

[19] G. P. Haber, M. A. White, R. Autorino, P. F. Escobar, M. D. Kroh, S. Chalikonda, R. Khanna, S. Forest, B. Yang, F. Altunrende, R. J. Stein, and J. H. Kaouk, "Novel Robotic da Vinci Instruments for Laparoendoscopic Single-site Surgery," *Urology*, Vol. 76, Issue 6, pp. 1279-82, 2010.

[20] Y. Kim, S. Cheng, S. Kim, and K. Iagnemma, "A Stiffness-Adjustable Hyper-Redundant Manipulator using a Variable Neutral-line Mechanism for Minimally Invasive Surgery," *IEEE Transactions on Robotics*, submitted, 2013.